



Thermophysical properties of the parylene C dimer under vacuum

Yamada, Monamie
Koshiha, Yasuko
Horike, Shohei
Fukushima, Tatsuya
Ishida, Kenji

(Citation)

Japanese Journal of Applied Physics, 59(SD):SDDA15-SDDA15

(Issue Date)

2020-03-01

(Resource Type)

journal article

(Version)

Version of Record

(Rights)

© 2020 The Japan Society of Applied Physics.

Content from this work may be used under the terms of the Creative Commons Attribution 4.0 license. Any further distribution of this work must maintain attribution to the author(s) and the title of the work, journal citation and DOI.

(URL)

<https://hdl.handle.net/20.500.14094/90007366>



REGULAR PAPER • OPEN ACCESS

Thermophysical properties of the parylene C dimer under vacuum

To cite this article: Monamie Yamada *et al* 2020 *Jpn. J. Appl. Phys.* **59** SDDA15

View the [article online](#) for updates and enhancements.



Thermophysical properties of the parylene C dimer under vacuum

Monamie Yamada¹, Yasuko Koshiba¹, Shohei Horike^{1,3}, Tatsuya Fukushima¹, and Kenji Ishida^{1,2*}

¹Department of Chemical Science and Engineering, Graduate School of Engineering, Kobe University, 1-1 Rokkodai-cho, Kobe, Hyogo, 657-8501, Japan

²Research Center for Membrane and Film Technology, Kobe University, Kobe 657-8501, Japan

³Nanomaterials Research Institute, National Institute of Advanced Industrial Science and Technology (AIST), 1-1-1 Higashi, Tsukuba 305-8565, Japan

*E-mail: kishida@crystal.kobe-u.ac.jp

Received August 9, 2019; revised October 25, 2019; accepted November 19, 2019; published online January 3, 2020

Herein, we report the thermophysical properties of dichloro-[2,2]-paracyclophane (the parylene C dimer) under vacuum. The parylene C dimer is the raw material used to prepare parylene C, a thin film known for its useful dielectric and barrier properties. In order to investigate the first step in the synthesis of parylene C by chemical vapor deposition, the sublimation, evaporation, and melting behavior of the parylene C dimer was examined by simultaneous thermogravimetry/differential thermal analysis (TG-DTA) under vacuum and at atmospheric pressure. The evaporation onset temperatures, saturation vapor pressures, and the phase-transition temperatures of the parylene C dimer were quantified by TG-DTA at various pressures. The evaporation and sublimation temperature easily decreased by increasing the level of vacuum, while the melting temperature was independent of the external pressure. Our results led to the construction of a pressure-temperature phase diagram.

© 2020 The Japan Society of Applied Physics

1. Introduction

Poly(*p*-xylylene), discovered by Szwarc¹⁾ and often referred to by its trade name “parylene”, is a polymer that possess useful dielectric and barrier properties. Its key properties include its mechanical strength, optical transparency, low permeability, high electrical insulating behavior, chemical stability, and biocompatibility.²⁻⁴⁾ Parylene is used as a gate dielectric in organic field-effect-transistors⁵⁾ and for the fabrication of medical electronics in a number of applications.⁶⁻⁸⁾ There are several types of parylene that differ by the substituents on the benzene ring and exhibit different coating properties. The most frequently used parylene is parylene C [poly(monochloro-*p*-xylylene)] in which one of the aromatic hydrogen atoms on each benzene ring is replaced by a chlorine atom.^{9,10)} Parylene C exhibits a good balance between mechanical and electronic characteristics; it can also be deposited more rapidly compared to others in the family.

Parylene C is deposited as pinhole-free films as thin as 50 nm¹¹⁾ by chemical vapor deposition. This process, known as the ‘Gorham process’,¹²⁻¹⁴⁾ starts with the sublimation of dichloro-[2,2]-paracyclophane (the parylene C dimer) at approximately 150 °C. The parylene C dimer gas is then pyrolyzed into the reactive monomer at high temperatures of between 600 °C and 700 °C. These monomers are transported into the deposition chamber, which is held at room temperature and where polymerization occurs as monomer radicals are deposited on a substrate. This polymerization process is mostly performed at a vacuum of around 20 Pa.

Research into the characteristics of parylene C, such as its mechanical, electronic, and biocompatibility properties, and how they relate to the thickness and the vapor-phase polymerization conditions has been reported.¹⁵⁻¹⁷⁾ There have also been studies into surface modifications using techniques such as plasma etching^{18,19)} and annealing,²⁰⁾ which were aimed at improving the above-mentioned qualities such that they meet application standards. However, studies devoted to the raw material itself, namely the parylene C dimer, are less

reported.^{21,22)} In particular, to the best of our knowledge, there are no studies that focus on the thermophysical properties of the dimer under vacuum, despite the fact that dimer vaporization is the first step toward the formation of parylene. Analyzing thermophysical properties under vacuum is difficult; however Takahashi et al. measured the saturation pressures of low-molecular-weight organic compounds by evacuated TG experiments^{23,24)} and Yase et al. measured evaporation rates of functional organic compounds by quadrupole mass spectrometry.^{25,26)} We have also reported the thermal behavior of ionic liquids and organic compounds under vacuum in our previous work.^{27,28)} With this in mind, it should be possible to examine the thermal properties of the parylene C dimer by thermogravimetry/differential thermal analysis (TG-DTA) under vacuum.

In this study, we focused on the sublimation and evaporation behavior of the parylene C dimer because it is the first step in the formation of parylene C by chemical vapor deposition. We examined the sublimation, evaporation, and melting behavior of the parylene C dimer by TG-DTA, from atmospheric pressure to 10⁻⁴ Pa, and determined its weight-loss onset temperatures, saturation vapor pressures, melting temperatures, evaporation temperatures, and sublimation temperatures. Moreover, we studied the phases of the parylene C dimer under vacuum and constructed a pressure-temperature (*P-T*) phase diagram.

2. Experimental methods

2.1. Materials

Dichloro-[2,2]-paracyclophane was purchased from Daisan Kasei; its chemical structure is shown in Fig. 1(b). Along with that of parylene C [Fig. 1(a)], Eicosane (C₂₀H₄₂) and anthracene (C₁₄H₁₀) were purchased from Tokyo Chemical Industry and Nacalai Tesque, respectively. All chemicals were used without further purification.

2.2. Setup and analysis

We used a modified Advance Riko VAP-9000 system for TG-DTA experiments. The system was fitted with a full



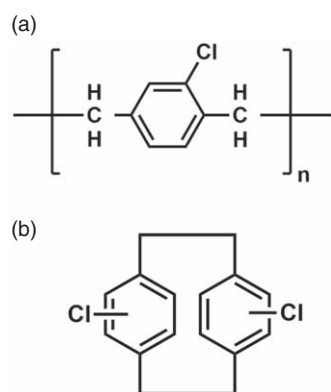


Fig. 1. Chemical structures of (a) the parylene C dimer and (b) parylene C.

range combined cold cathode and pirani gauge by Pfeiffer Vacuum, a rotary pump, and an oil diffusion pump in order to examine evaporation behavior in the 10^{-4} Pa to atmospheric pressure range. For pressures lower than 10^{-1} Pa, we used the oil diffusion pump and for higher pressures we used the rotary pump. By choosing which pump and adjusting the closure of the valve that connects the pump and the chamber, we controlled the pressure range. The external pressure of the chamber was measured by the vacuum gauge put in between the pump and chamber. As apparatus constants for our setup, coagulation factors α : (the degrees of evaporation hampering by residual gas molecules), which are required for calculating saturation vapor pressures, were determined in preliminary experiments using eicosane and anthracene. Sample weight losses were monitored and DTA was performed while samples were heated in an aluminum cell at 2°C min^{-1} from room temperature, with an empty cell used as a reference.

3. Results and discussion

The TG curves for the parylene C dimer under a variety of external pressures are shown in Fig. 2(a). The external pressures are measured at the start of the heating and range in less than 10% throughout the experiment on the average. However, at higher vacuumed environment, pressures ranged up to 40% (4.4×10^{-4} – 6.0×10^{-4} Pa) from the start. Higher vacuums were observed to shift the TG curves to lower temperatures, with the amount of displacement lower at pressures below 10^{-1} Pa. To explain the shifting of the TG curves with numbers, we defined the weight-loss onset temperature as the temperature where the initial weight decreased by 5%. As shown in Fig. 2(b), the onset temperature declined from 169.5°C at atmospheric pressure to 58.6°C at 10^{-4} Pa. At lower external pressures, the number of residual gas molecules in the air; such as nitrogen, oxygen, water, decreases. As the dimer sublimates/evaporates, the dimer molecules also fill the chamber changing the component of residual gas molecules. However at the beginning of sublimation/evaporation, the components can be thought to be only the atmosphere, explaining how molecules easily sublime/evaporate at lower external pressures. Also, with less residual gas molecules to obstruct, the mean free path becomes longer. The evaporation/sublimation behavior at the interface between solid/liquid and gas will complicatedly change depending on the degree of vacuum.

We concurrently acquired DTA curves, as shown in Fig. 2(c). Two endothermic peaks are evident in the

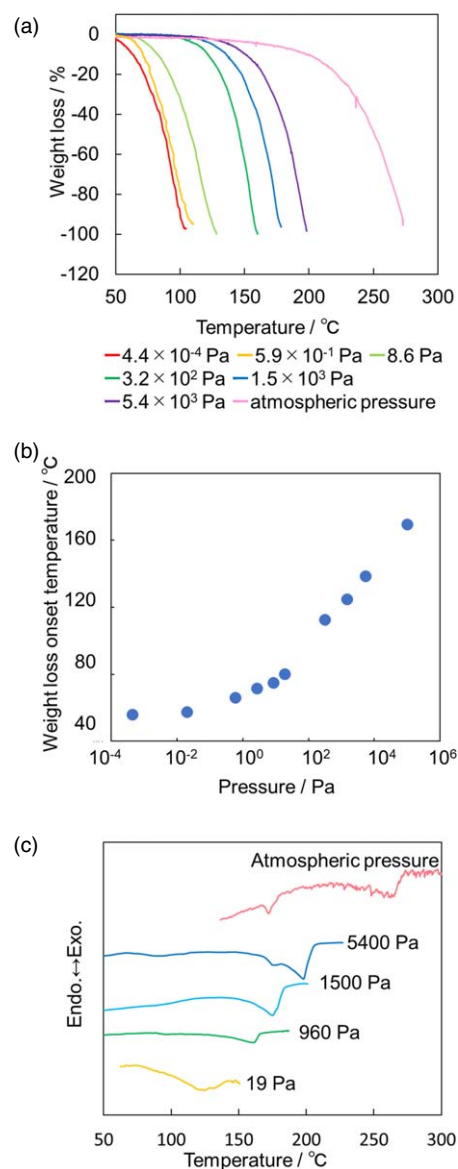


Fig. 2. (Color online) (a) TG curves, (b) weight-loss onset temperatures, and (c) DTA curves of the parylene C dimer at various vacuum levels.

atmospheric pressure to 10^2 Pa range, which indicates that the parylene C dimer melts and evaporates at low vacuum. By combining these results with those obtained by TG, we determined whether or not weight is simultaneously lost through this endothermic process. The peaks observed at lower temperatures are attributed to melting because they are not associated with weight-loss. On the other hand, the peaks at higher temperatures are associated with weight-loss, consistent with dimer evaporation that leaves the pan empty. Only single endothermic peaks were observed at 960 and 19 Pa. According to the TG results, these peaks are associated with weight-loss, which indicates that the dimer sublimates under the various vacuum conditions. The two endothermic peaks almost overlap at 1500 Pa, suggestive of a phase-transition triple point. The temperature at which the melting peak first appears (hereinafter referred to as the melting temperature, T_m) is independent of pressure in the 165°C – 170°C range. However, the temperatures at which the evaporation (T_e) and sublimation (T_s) peaks appear decrease with increasing the degree of vacuum, which is the same trend observed for the TG curves. The reason why T_m is less

pressure dependent than either T_e or T_s is provided by the following Clausius–Clapeyron equation:

$$\frac{dT}{dP} = \frac{T(V_\beta - V_\alpha)}{\Delta H}. \quad (1)$$

In Eq. (1) P is pressure, T is the temperature, V_α and V_β are the volumes before and after phase-transition, and ΔH is the phase-transition enthalpy change. Compared to evaporation and sublimation, a smaller volume change is observed when solids melt and become liquids, which results in a small dT/dP and a small difference in T_m with changing pressure. In addition, weight-loss is observed to commence at a temperature below the melting point at atmospheric pressure, which shows that the parylene C dimer is an easy-to-sublime substance.

To elucidate the details of the first step in the formation of parylene C, which is the sublimation/evaporation of the parylene C dimer, we analyzed the TG data using the Hertz–Knudsen–Langmuir and Clausius–Clapeyron equations. The saturation vapor pressure (p) is expressed as follows:^{23,27)}

$$p = \frac{r}{\alpha} \sqrt{\frac{2\pi RT}{M}}. \quad (2)$$

Here, r is the sublimation/evaporation rate, M is the molecular mass, R is the gas constant, and α is the coagulation factor ($0 < \alpha \leq 1$), which represents the degree of evaporation hampering by residual gas molecules and is an apparatus constant that depends on the external pressure. The value of α is believed to asymptotically approach unity at high degree of vacuum because the number of residual gas molecules decreases. Values of α were determined beforehand in preliminary experiments, as described below.

According to the Clausius–Clapeyron equation, the external pressure and boiling temperature are related as described by Eq. (3):

$$\ln\left(\frac{p_2}{p_1}\right) = -\frac{\Delta H}{R}\left(\frac{1}{T_2} - \frac{1}{T_1}\right). \quad (3)$$

Here T_1 and T_2 are the evaporation points at external pressures p_1 and p_2 , and ΔH is the evaporation enthalpy. We selected eicosane, (molecular weight: 282.55, evaporation point: 343.1 °C, evaporation enthalpy: 102 kJ mol⁻¹²⁹⁾) and anthracene (molecular weight: 178.23, evaporation point: 340 °C, evaporation enthalpy: 100 kJ mol⁻¹³⁰⁾) for use in preliminary experiments to determine α . The evaporation points at each external pressure were calculated by substituting known evaporation points at atmospheric pressure and the evaporation enthalpies into Eq. (3). We next subjected eicosane and anthracene to TG at various external pressures. Evaporation rates were calculated, along with the molecular weights and estimated evaporation points determined at external pressures, to provide α values. The values of α for both eicosane and anthracene are shown in Fig. 3; α clearly asymptotically approaches unity with increasing the level of vacuum. The α values of these two materials are similar, which confirms that α is a consequence of residual gas molecules such as nitrogen, oxygen and water rather than molecules undergoing evaporation. Based on these results we conclude that these α values are suitable for the parylene C dimer, and we consistently used the values calculated from eicosane.

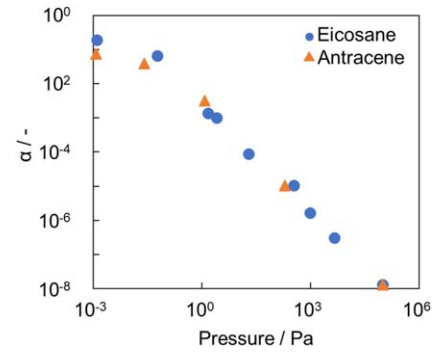


Fig. 3. (Color online) Coagulation factor (α) determined by TG experiments involving eicosane and anthracene at various vacuum levels. We consistently used α determined for eicosane in further discussions.

The saturation vapor pressure of the parylene C dimer was calculated using Eq. (2) and the TG data at various external pressures; the saturation vapor pressures at external pressures of 10^{-4} Pa, 960 Pa, and atmospheric pressure are shown in Figs. 4(a)–4(c), respectively. The saturation vapor pressure curves shift to lower temperatures with decreasing external pressure. Weight-loss onset temperatures where the saturation vapor pressures started to increase. We defined the sublimation/evaporation point as the temperature at which the saturation vapor pressure is equal to the external pressure, as shown by the dotted lines in Figs. 4(a)–4(c).

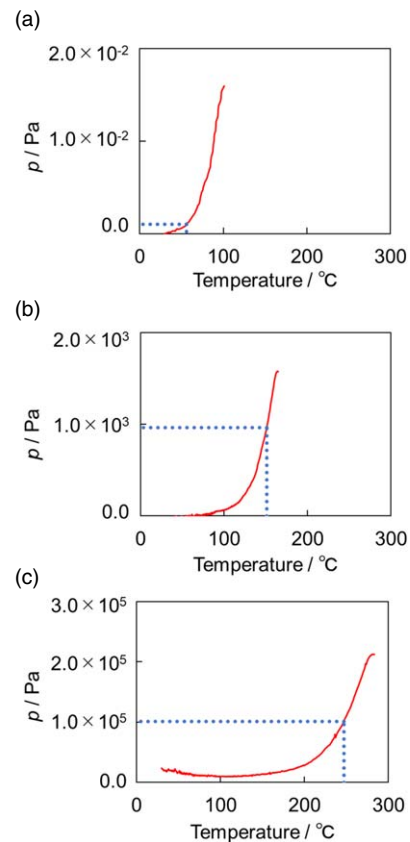


Fig. 4. (Color online) (a) Saturation vapor pressures as functions of temperature at external pressures of (a) 1.0×10^{-3} Pa, (b) 960 Pa, and (c) atmospheric pressure obtained from the TG data and the Hertz–Knudsen–Langmuir equation using the coagulation factors calculated from preliminary experiments. The dotted lines show the temperatures of sublimation/evaporation points, where saturation vapor pressures are equal to external pressures.

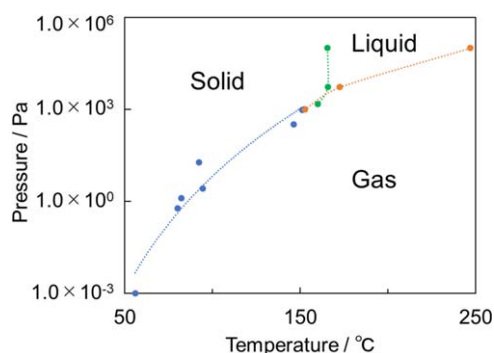


Fig. 5. (Color online) Pressure-temperature (P - T) phase diagram for the parylene C dimer constructed from the experimental TG-DTA results.

Finally, we constructed a P - T phase diagram for the parylene C dimer (Fig. 5) using the experimental TG-DTA data, by plotting T_s , T_m , and T_e calculated from the TG-DTA experiments. This diagram clearly reveals that the parylene C dimer sublimates at 120 °C at 20 Pa, and parylene C is generally deposited under these conditions.

4. Conclusion

We studied the thermophysical behavior of the parylene C dimer under vacuum by TG together with theoretical analyses. The weight-loss onset temperature decreases and the dimer readily sublimates with increasing vacuum level. The dimer melts at 165 °C–170 °C and evaporates at higher temperatures at pressures above 1500 Pa. The melting temperatures are independent of the external pressures, but the evaporation temperature decreases with increasing the level of vacuum. Based on these results, we constructed a P - T phase diagram for the parylene C dimer. We believe that this study provides concise information for the chemical vapor deposition of parylene C because the first step in this process involves sublimation of the dimer. This information may lead to conditions for efficiently depositing parylene C with required properties in the future.

Acknowledgments

This study was partially supported by JSPN KAKENHI and JST CREST.

- 1) M. Szwarc, *Discuss. Faraday Soc.* **2**, 46 (1947).
- 2) S. Biswas, O. Shalev, K. P. Pipe, and M. Shtein, *Macromolecules* **48**, 5550 (2015).
- 3) Y. H. Lei, Y. P. Liu, W. Wang, and W. G. Wu, *Lab Chip* **11**, 1385 (2011).
- 4) J. J. Senkevich, G.-R. Yang, and T.-M. Lu, *Colloids Surf. A* **216**, 167 (2003).
- 5) I. Tsydel, T. Marszalek, J. Ulanski, A. Nosal, and M. Gazicki-Lipman, *Surf. Coat. Technol.* **290**, 21 (2016).
- 6) S. Kuppusami and R. Oskoue, *Univers. J. Biomed. Eng.* **3**, 9 (2015).
- 7) S. Takeuchi, D. Ziegler, Y. Yoshida, K. Mabuchi, and T. Suzuki, *Lab Chip* **5**, 519 (2005).
- 8) E. G. R. Kim, J. K. John, H. Tu, Q. Zheng, J. Loeb, J. Zhang, and Y. Xu, *Sens. Actuators B* **195**, 416 (2014).
- 9) W. F. Beach, in *Encyclopedia of Polymer Science and Technology*, ed. H. F. Mark (Wiley, New York, 2004).
- 10) B. Lu, Z. Yin, H. Zou, L. Zhi, and J. Feng, *Mater. Sci. Semicond. Process.* **40**, 811 (2015).
- 11) W. Leventon and M. Dev, *Diagn. Ind.* **2001**, 48 (2001).
- 12) W. F. Gorham, *J. Polym. Sci., Part A* **4**, 3027 (1966).
- 13) J. B. Fortin and T.-M. Lu, *Chemical Vapor Deposition Polymerization: The Growth and Properties of Parylene Thin Films* (Kluwer Academic Publishers, Norwell, MA, 2004) 1st ed., Chap. 1.
- 14) L. A. Errede and M. Szwarc, *Quart. Rev.* **12**, 301 (1958).
- 15) S. Bourlidi, J. Qureshi, S. Soo, H. Petridis, and C. Prosthod, *J. Prosthet. Dentistry* **115**, 363 (2016).
- 16) M. A. Spivack, *Rev. Sci. Instrum.* **41**, 1614 (1970).
- 17) G. E. Loeb, M. J. Bak, N. Salcman, and E. M. Schmidt, *IEEE Trans. Biomed. Eng.* **24**, 121 (1977).
- 18) M. Golda-Cepa, M. Brzychczy-Wloch, K. Engvall, N. Aminlashgari, M. Hakkarainen, and A. Kotarba, *Mater. Sci. Eng. C* **52**, 273 (2015).
- 19) D. Kontziampasis, T. Trantidou, A. Regoutz, E. J. Humphrey, D. Carta, C. M. Terraciano, and T. Prodromakis, *Plasma Processes Polym.* **13**, 324 (2016).
- 20) N. Jackson, F. Stam, J. O'Brien, L. Kailas, A. Mathewson, and C. O'Murchu, *Thin Solid Films* **603**, 371 (2016).
- 21) J. Lahann, *Polym. Intern.* **55**, 1361 (2006).
- 22) M. Cetinkaya, N. Malvadkar, and M. C. Demirel, *J. Polym. Sci., Part B* **46**, 640 (2008).
- 23) Y. Takahashi, K. Matsuzaki, M. Iijima, E. Fukuda, S. Tsukahara, Y. Murakami, and A. Maesono, *Jpn. J. Appl. Phys.* **32**, 875 (1993).
- 24) K. Yase, Y. Takahashi, N. Ara-Kato, and A. Kawazu, *Jpn. J. Appl. Phys.* **34**, 636 (1995).
- 25) K. Yase and Y. Yoshida, *Jpn. J. Appl. Phys.* **34**, 3903 (1995).
- 26) K. Yase, Y. Yoshida, T. Uno, and N. Okui, *J. Cryst. Growth* **166**, 942 (1996).
- 27) S. Horike, M. Ayano, M. Tsuno, T. Fukushima, Y. Koshiba, M. Misaki, and K. Ishida, *Phys. Chem. Chem. Phys.* **20**, 21262 (2018).
- 28) Y. Koshiba, M. Nishimoto, A. Misawa, M. Misaki, and K. Ishida, *Jpn. J. Appl. Phys.* **55**, 03DD07 (2015).
- 29) J. S. Chickos and W. Hanshaw, *J. Chem. Eng. Data* **49**, 620 (2004).
- 30) V. Oja and E. M. Suuberg, *J. Chem. Eng. Data* **43**, 486 (1998).